Numerical Methods in Civil Engineering

Damping of Steel Eccentrically Braced Frames in Direct Displacement-Based Design

Bahram Rezayibana* and Mahmood Yahyai**

ARTICLE INFO

Article history:
Received:
January 2018.
Revised:
May 2018.
Accepted:
June 2018.

Keywords:
Damping, Displacement Ductility, Eccentrically Braced Frame

Abstract:

Due to the limitations and deficiencies in the force-based design approach, several methods are introduced and examined in order to improve this methodology. However, over the years, researchers have proposed displacement-based design methods. Among them, the direct displacement-based design (DDBD) method is one of the most thorough and accepted. The main goal of this method is to determine equivalent damping. Considering the equivalent damping and target displacement corresponding to the desired ductility, the design base shear is obtained from the displacement spectrum. Several methods are proposed to determine equivalent damping. In this study, the revised effective mass (REM) method is employed for the design of eccentrically braced frame (EBF) systems. Using this method, equivalent damping is determined for EBF's. An expression is proposed for determining the equivalent damping for EBF's in term of ductility.

1. Introduction

In the force-based design method, sections are designed in a way that in all stories link beams reach their yielding capacity. This approach is also referred to as force-control design. In this method, the base shear is distributed linearly in height with respect to the first shape mode. However, it is possible that the inter-storey drift controls the design. Therefore, the direct displacement based design method was introduced to address this issue. Furthermore, in the force-based seismic design, the structure is modelled based on the elastic properties and the effects of yielding are neglected. On the other hand, in DDBD approach, the structure is modelled based on the secant stiffness evaluated at the maximum displacement, Δ_d, for a given equivalent damping, accounting for elastic and hysteretic damping in the nonlinear response. This method is a performance-based design method which was introduced by Priestley [1] for the first time for designing RC structures. Figure 1, shows the direct displacement based design procedure.

** Corresponding Author: Assistant Professor, Department of Civil Engineering, Ardabil Branch, Islamic Azad University, Ardabil, Iran, Email: Bahram.deprem@gmail.com.*

*** Adjunct Professor, Civil Engineering Department, School of Engineering, Morgan State University, Baltimore, Maryland, USA*

In DDBD procedure, a frame building is represented as a single-degree-of-freedom system (SDOF). By considering a design displacement equal to the maximum response of a SDOF and the corresponding ductility, the equivalent viscous damping(ζ_{eq}) is calculated. Then, the structure period (T_e) is determined from the displacement spectrum at the equivalent viscous damping. Afterwards, the structures stiffness (K_e) is calculated by equation 1 for a given effective mass (m_e). By multiplying the stiffness in the design displacement, the design base shear (V_{base}) is determined by equation 2.

$$K_e = 4\pi^2 \frac{m_e}{T_e^2} \quad (1)$$

$$F = V_{base} = K_e \Delta_d \quad (2)$$

The DDBD method was first developed to design SDOF systems considering the substitute structure concept [1]. This method was then employed to design concrete bridges [2]. Calvi and Kingsley (1995), Kowalsky (2002) Priestley and Calvi (2003) extended this method to multi-span bridges[3-5]. Moreover, this method was evaluated for designing long span bridges by Adhikari et al. (2010) and it was modified by conducting parametric studies[6]. Calvi

and Pavese (1995)[7] presented a formulation for designing RC structures, which was then modified by Priestley [8]. This method was extended by Harris (2004) for moment-resisting system, Yavas (2006) for shear-wall system, Garcia et al. (2010) for dual system (moment-resisting and shear wall), Wijesundara et al. (2011) for concentrically braced frame (CBF) and Yahyai and, Rezayibana (2017) for special concentrically braced frame (SCBF)[9-13].

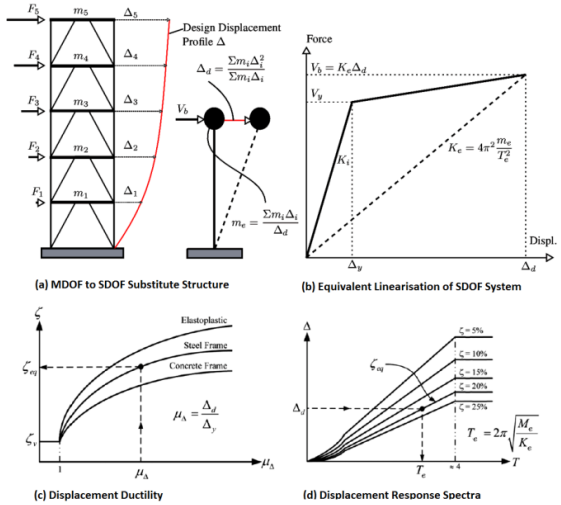

Fig. 1: Direct displacement based design procedure

As discussed earlier, the most important parameter of the DDBD is the equivalent viscous damping. The equivalent viscous damping is the sum of the elastic damping and the hysteretic damping of an equivalent SDOF system($\zeta_{eq} = \zeta_{el} + \zeta_{hys}$). The equivalent viscous damping depends on the structural system, ductility(μ), the elastic damping and whether it is defined based on the initial stiffness or the secant stiffness. It is necessary to select a ductility level for designing a structure, whether for the entire structure or specific elements. Then, by using relationships or equivalent damping charts derived based on ductility and structural system, the equivalent viscous damping for an SDOF system is determined. Jacobsen (1960) conducted research on evaluation of the equivalent viscous damping[14]; however, the assumptions made in his proposed method do not lead to accurate results[15]. Grant et al. (2005) and Dwairi et al. (2007) put in more atempted to address the problem associated with Jacobsen's method[16-17]. Dwairi et al. (2007) calculated the equivalent viscous damping for a large number of earthquake accelerograms with different ductility levels and effective periods. Eventually, by averaging over different cases, a relationship for the equivalent viscous damping was derived for different hysteresis curves as a function of ductility. In this method, after determining the yield displacement and the target displacement with respect to the desired ductility, the hysteretic damping is evaluated by employing the Jacobsen method. Then, the effective period of the system is determined from the inelastic displacement spectrum at the hysteretic damping value. Afterwards, the effective mass and stiffness are calculated and nonlinear time historey analysis is carried out. Convergence is achieved if the displacement obtained by the analysis and the target displacement are identical. Otherwise, another value for damping is assumed and this procedure is repeated until convergence occurs and the final damping value is taken as the equivalent viscous damping. They proposed equation 3 denoted here as standard expression to estimate the equivalent viscous damping of steel frames.

$$\zeta_{eq} = 0.05 + 0.577\frac{\mu - 1}{\pi\mu} \qquad (3)$$

One drawback of this method is the large number of frequent references of the displacement spectrum. Yahyai and Rezayibana (2015) proposed the revised effective mass (REM) method to reduce the computational effort of Dwairi's method[18]. This method is shown in figure 2.

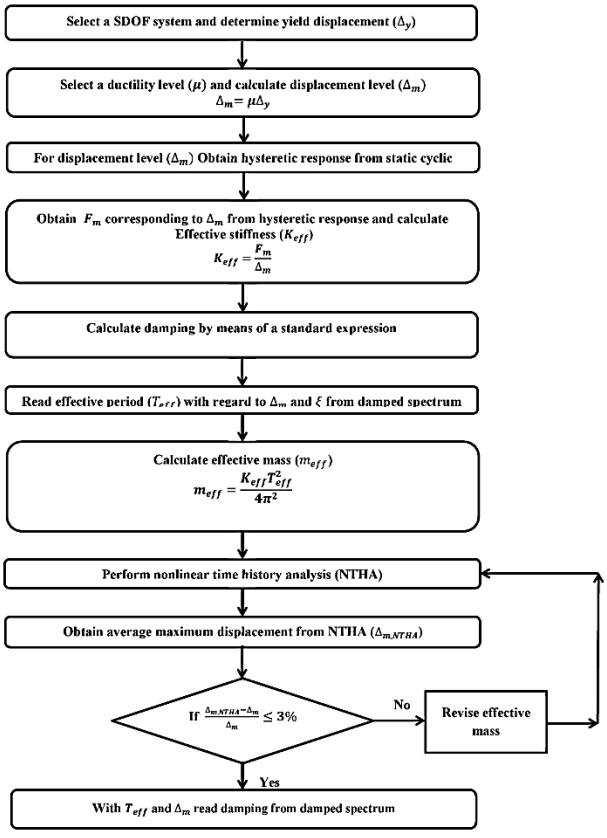

Fig. 2: Flow chart of REM methodology[18]

In this paper, this approach is used to estimate the equivalent damping of eccentrically braced frames (EBFs). In this regard, eight EBFs are designed according to AISC (2016)[19] and then analyzed in order to evaluate the equivalent damping based on the REM methodology. This

study proposes an expression for estimating the equivalent damping, based on the ductility level for EBF's.

2. Design Cases

Eccentrically braced frame (EBF) is a ductile system for resisting lateral loads in seismic regions. In this system, the energy induced by the earthquake is absorbed by developing plastic hinges in the link beam, while the rest of the system including columns, outer beam segments and braces remain in the elastic range. In fact, the link beam acts as a fuse in the bracing system. Link beams are divided into three types based on their length(e):

1- Short link beam with shear yielding mechanism ($e < 1.6\frac{M_p}{V_p}$)

2-Medium link beam with shear - flexural yielding mechanism ($1.6\frac{M_p}{V_p} < e < 2.6\frac{M_p}{V_p}$)

3- Long link beams with flexural yielding mechanism ($e > 2.6\frac{M_p}{V_p}$)

Where e is the link length, V_p and M_p denote plastic shear and plastic moment of the link beam calculated by equations 4 and 5, respectively[19].

$$V_p = \begin{cases} 0.6\, F_y\, A_{lw} & \frac{P_r}{P_y} \le 0.15 \\ 0.6\, F_y\, A_{lw}\sqrt{1-\left(\frac{P_r}{P_y}\right)^2} & \frac{P_r}{P_y} > 0.15 \end{cases} \quad (4)$$

$$M_p = \begin{cases} F_y\, Z & \frac{P_r}{P_y} \le 0.15 \\ F_y\, Z\left(\frac{1-\frac{P_r}{P_y}}{0.85}\right) & \frac{P_r}{P_y} > 0.15 \end{cases} \quad (5)$$

Where P_r, P_y, F_y, Z, and $A_{lw}$are the required axial strength, the nominal axial yield strength, the yield stress, the plastic module and the web section area of the link beam, respectively. In order to evaluate the equivalent damping for eccentrically braced frames, eight single storey frames with 5m storey height and 5m width of the bay were designed in accordance with AISC (2016) based on the link beam capacity. The length of the link beam was selected such that it included all types of link beam actions. W8x8x18 section was selected for the link beam. In EBF systems, link beam acts as a fuse and it reaches its yield capacity, while other members remain elastic. To attain this aim, the plastic capacity of other members was taken to be 25 percent higher than the link beams. Regarding the link beam section, in order to encompass all link beam mechanisms, link beams with the length of 300 mm, 500 mm (shear mechanism), 700 mm (shear-flexural) and 900 mm, 1100 mm, 1500 mm, 2000 mm and 2500 mm (flexural) were considered. Since the link beam section was constant and the length of link beam was variable, other members were designed such that they satisfied the plastic capacity equal to 1.25 times the capacity of link beam and remained unchanged in this study. W8x8x21 and HSS5x5x1/4 sections were designd for the columns and braces, respectively.The nominal yield stress(F_y) and the Young's modulus of the steel(E) were taken as 350MPa and 200GPa, respectively.

3. Numerical Modeling and Verification

All Frames were modeled using ABAQUS software[20]. Members were modelled using 3D shell elements (S4R). This element is used to model both thin and thick shells and it is capable of modeling plasticity, creep, inflation, strain hardening and large deformations. All members except the beam were merged. In order to model the hinge connection between column and beam, a coupling connection in the section plane was defined and these connections were joined together. Moreover, the hinge connection at the base was modelled by defining a coupling connection at a reference point at 20 mm distance from the end of columns and the support conditions were defined such that only the rotation in the frame plane was allowed. Furthermore, out of the plane movement was cancelled by constraining columns and beams in that direction. In order to model the steel material behavior, a bilinear elasto-plastic behavior with 1 % strain-hardening was adopted. For cyclic analysis, a displacement time history with the amplitude of the target displacement corresponding to the desired ductility was applied at the top of the frames. Figure 3, shows the model of the frame in ABAQUS.

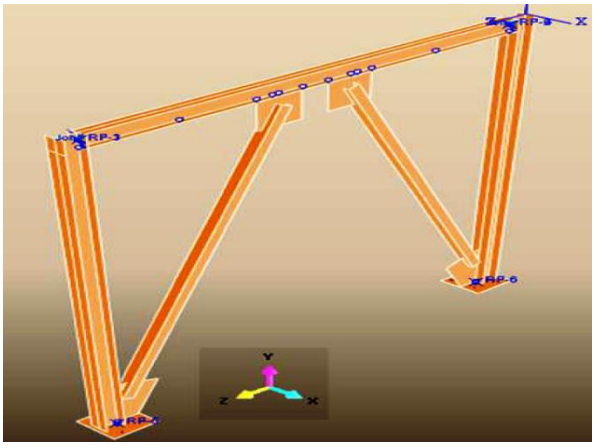

Fig. 3: Numerical model of EBF

In order to verify the numerical model, the EBF model tested by Berman and Bruneau(2007) was used[21]. The test setup is shown in figure 4. As shown, the frame dimensions were set to a height of 3150 mm and width of 3660 mm. the length of link beam was set to 456 mm. A hydraulic actuator applied horizontal force to a loading beam at the top of the frame. Figure 5 shows a comparison

between experimental and the numerical model results. As shown, the overall hysteretic response is well predicted by the numerical model.

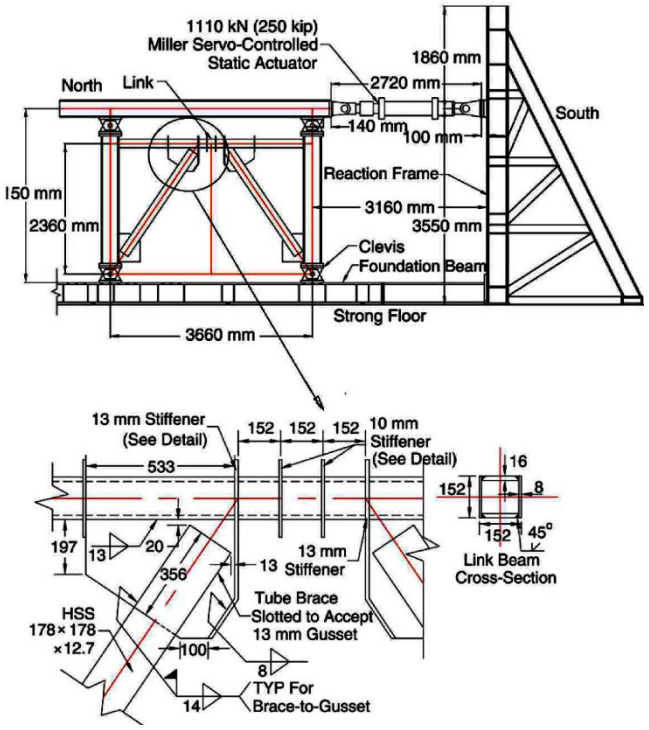

Fig. 4: Test setup(Berman and Bruneau,2007) [21]

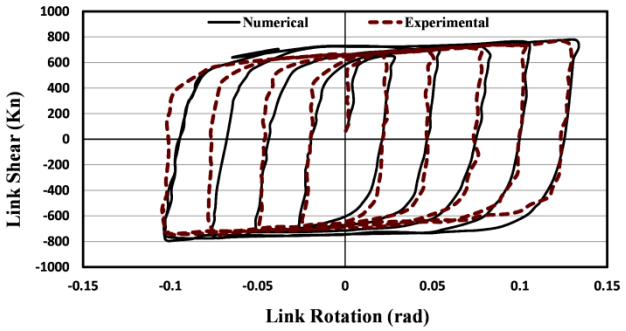

Fig. 5: Comparison of hysteresis response of numerical and experimental results

4. Jacobsen Hysteretic Damping

Jacobsen assumed that the velocity of the equivalent SDOF system is equal to the velocity of the real structure. Equating the dissipated energy by a nonlinearly damped elastic SDOF to an elastic SDOF using the hysteretic damping under a sinusoidal excitation, leads to equation 6.

$$\zeta_{hys} = \frac{A_h}{2\pi F_m \Delta_m} \tag{6}$$

Where, A_h is the area of a complete hysteresis force-displacement response, F_m denotes the maximum force and Δ_m is the displacement corresponding to F_m. In this study, for calculating the hysteretic damping by Jacobsen method, a sinusoidal displacement history with the amplitude of the target displacement corresponding to the desired ductility is applied and A_h is evaluated for a loop in the force-displacement curve. Then, by determining the maximum force and the corresponding displacement, the hysteretic damping is calculated by equation 6. It should be noted that, by Jacobsen's method, the most effective parameters on damping are determined.

In accordance with equation 3, ductility is the most important parameter for estimating the hysteretic damping. Ductility is defined as the ratio of target displacement to yield displacement. The elastic displacement of an EBF storey can be computed by summing the displacements caused by the deformations of individual components of the frame. With an elastic analysis, a relationship was presented to determine the yield displacement for an EBF system. The yield displacement (Δ_y) is estimated by equation 7.

$$\Delta_y = \Delta_{br} + \Delta_{Vlink} + \Delta_{Mlink} \tag{7}$$

Where Δ_{br}, Δ_{Vlink} and Δ_{Mlink} are the individual lateral displacements of the EBF due to brace axial deformation, link shear deformation and link flexural deformations calculated by equations 8-10, respectively. Deflections associated with column axial deformations are negligible for a single storey.

$$\Delta_{br} = \frac{F}{2E}\left(\frac{L_{br}}{A_{br}}\right)\left(\frac{L_{br}}{a}\right)^2 \tag{8}$$

$$\Delta_{Vlink} = \frac{F}{G}\left(\frac{h^2 e}{A_{Vlink} L^2}\right) \tag{9}$$

$$\Delta_{Mlink} = \frac{F}{E}\left(\frac{h^2 e^2}{12 I_{link} L}\right) \tag{10}$$

Where E and G are Young's and shear modulus of steel, respectively, A_{br} is the cross section area of the brace, A_{Vlink} and I_{link} are the shear area and the second moment of inertia of the link section, respectively and other terms are defined in figure 6.a. F is the lateral strength of an EBF defined according to figure 6.b and c. Since plastic shear and moment of the link govern in the case of shear and flexural link respectively. The lateral strength of EBF was defined based on the link strength (V_p or M_p).

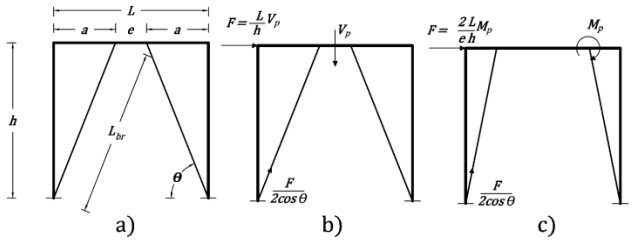

Fig. 6: a) EBF dimensions , b) lateral strength in the case of shear link and C) lateral strength in the case of flexural link

The yield displacements of the selected frames were calculated by equation 7 and then applied as cyclic loading. Based on Jacobsen's assumption, hysteretic damping corresponding to yield displacement is equal to zero. Since the accurate estimation of the displacement corresponding to the hysteretic damping equal to zero is not possible in finite element models, the yield displacements calculated by the proposed relationship were used to estimate the hysteretic damping. However, to insure that the yield displacements are calculated correctly, the hysteretic damping corresponding to the yield displacement or ductility level 1 should be less than 5%. It should be noted that, in most references this criterion is used up to 5% [11-15]. The hysteretic damping of the frames at ductility level 1 is presented in Table 1.

Table 1. The yield displacement of the frames

length of the link (mm)	Yield displacement (mm)	Hysteretic Damping (%)
300	9.359	4.5
500	13.345	3
700	18.902	2.5
900	23.861	2.2
1100	26.072	1
1500	31.408	1.2
2000	38.990	1.3
2500	47.321	4

As can be seen, the yield displacement calculated by proposed equation is sufficiently accurate. In order to determine the hysteretic damping, ten ductility levels were considered. For each ductility level, the maximum displacement $\Delta_m = \mu\Delta_y$was calculated and applied to every frame as a lateral cyclic loading. The hysteretic response of base shear-top lateral displacement was obtained and the hysteretic damping was determined by equation 6. Figure 7 shows the hysteretic damping values for frames with different link length to span length ratios.

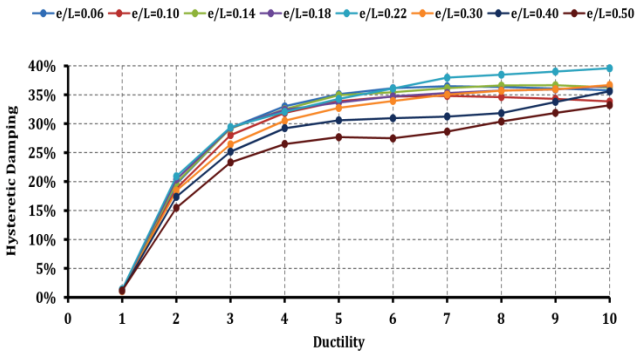

Fig. 7: The hysteretic damping of the frames against ductility

As seen in figure 7, the hysteretic damping depends on ductility level and the link length to the span length ratio. As the ductility level is increased, the damping is also increased. The hysteretic damping is approximately same for the frames with the link length to the span length ratio less than 0.3. For the frames with the link length to the span length ratio of 0.4 and 0.5, where the link beam is very long and the beam-bracing connection is close to the beam-column connection, the rigidity in the beam-column connection is increased and the frame mechanism is changed to moment frame. Since such behavior is not desirable for EBF's, these two models are no longer considered in this paper. It is recommended that the link length to the span length ratio could be selected less than 0.3 for designing EBF systems.

5. Effective Stiffness

One of the most important parameters in direct displacement based design method is the effective stiffness (K_{eff}) which is the key parameter in determining the effective period and the design base shear. After conducting cyclic analyses and obtaining the force-deformation curve, the effective stiffness is calculated by equation 11.

$$K_{eff} = \frac{F_m}{\Delta_m} \tag{11}$$

The normalized stiffness is defined as the ratio of the effective stiffness to the elastic stiffness (K_{eff}/K_{el}). Equation 12 is used to determine the elastic stiffness of EBF's.

$$\frac{1}{K_{el}} = \frac{1}{K_{br}} + \frac{1}{K_{Vlink}} + \frac{1}{K_{Mlink}} \tag{12}$$

Where K_{br}, K_{Vlink} and K_{Mlink} are the lateral stiffness of the brace due to axial stiffness, the lateral stiffness of the link due to shear stiffness and the lateral stiffness of the link due to flexural stiffness calculated by equations 13-15, respectively. The variation of the normalized stiffness for the frames is shown in figure 8.

$$K_{br} = 2E(\frac{A_{br}}{L_{br}})(\frac{a}{L_{br}})^2 \tag{13}$$

$$K_{Vlink} = G(\frac{A_{Vlink}L^2}{h^2 e}) \tag{14}$$

$$K_{Mlink} = E(\frac{12I_{link}L}{h^2 e^2}) \tag{15}$$

As shown in figure 8, the normalized stiffness depends only on the ductility and the link length to the span length ratio does not significantly influence normalized stiffness. Since the variation in the normalized stiffness against ductility for the different ratios are small, the average value is used. The average normalized stiffness is also shown in figure 8. Therefore, the normalized stiffness can be obtained by fitting an exponential curve to the normalized

stiffness. The effective stiffness is determined by equation 16.

$$K_{eff} = \frac{K_{el}}{\mu^{0.715}} \quad (16)$$

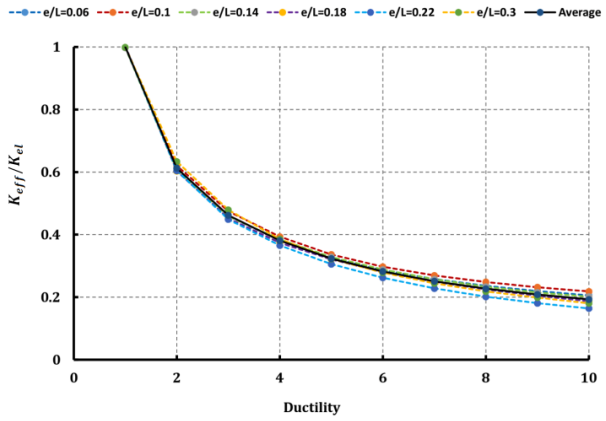

Fig. 8: Variation of the normalized stiffness against ductility

6. Ground Motion Selection

In order to determine the effective period and the equivalent damping used in the REM methodology for a given displacement level, a set of displacement spectrums based on different damping levels are required. To achieve this goal, ten real ground motions were selected for a given site class. In this study, site class C (very dense soil and soft rock) was assumed according to ASCE-7 (2016) [22]. To scale the selected ground motions, a design displacement spectrum with 5% damping was assumed. The corner period of the aforesaid spectrum for San Francisco was determined as six seconds. The characteristics of the selected ground motions and their scale factors are presented in Table 2. To assess the accuracy of the average spectrum, the design displacement spectrum for different damping levels is required. The displacement spectrum for different levels of damping was scaled by the scale factor presented by Priestley (2007)[23] as follows:

$$R_\zeta = \left(\frac{7}{2+\zeta}\right)^{0.5} \quad (17)$$

The average and design displacements spectrums which were compared and shown in figure 9 illustrate that, the average spectrum was also very close to the design spectrum for different damping levels.

Table 2. Ground motion database

Event	Year	Station	Mag	PGA (g)	Scale Factor
Imperial Valley	1977	Cerro Prieto	6.53	0.168	3.25
Imperial Valley	1979	Cerro Prieto	6.53	0.157	2.5
Tabas, Iran	1978	Dayhook	7.35	0.324	2.25
Loma Prieta	1989	APEEL 10 - Skyline	6.93	0.103	2.2
Loma Prieta	1989	APEEL 7 - Pulgas	6.93	0.108	2.5
Loma Prieta	1989	Anderson Dam (L Abut)	6.93	0.064	1.8
Loma Prieta	1989	Bear Valley #5_ Callens Ranch	6.93	0.068	3
Loma Prieta	1989	Berkeley LBL	6.93	0.118	3
Loma Prieta	1989	Coyote Lake Dam - Southwest Abutment	6.93	0.485	1.5
Loma Prieta	1989	Lower Crystal Springs Dam dwnst	6.93	0.089	2.75
Loma Prieta	1989	SF - Rincon Hill	6.93	0.168	3.25
Loma Prieta	1989	Point Bonita	6.93	0.157	2.5

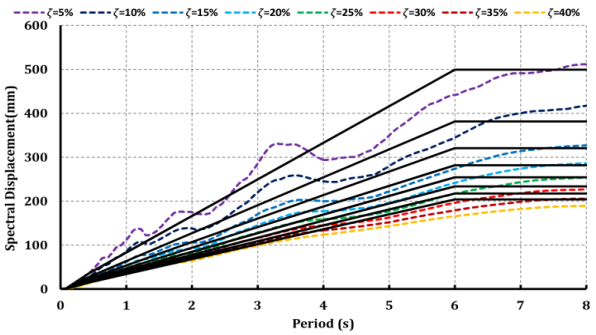

Fig. 9: The average and design displacements spectrums at different damping levels

7. Nonlinear time history analysis

The REM methodology was used for estimating hysteretic damping by means of a nonlinear time history analysis for EBFs. As shown in figure 2, the REM methodology is described as follows:

For each frame, the lateral yield displacement Δ_y is determined by equation 7. A ductility level is selected and then the maximum lateral displacement $\Delta_m = \mu\Delta_y$is calculated. The equivalent viscous damping ζ_{eq} is determined by equation 3. With $\Delta_m$and ζ_{eq}, the effective period is read from the average elastic response spectra at

the damping level by using figure 9. The elastic and effective stiffness are determined by equations 11and 16, respectively. Nonlinear time history analysis is performed using the ABAQUS software for the 10 selected records. The Newmark's average acceleration method and tangent stiffness proportional damping model with 5% critical damping were utilized in these analyses. To perform a nonlinear time history analysis, it is required that a mass be assigned, which is determined by equation 18.

$$m_{eff} = \frac{T^2}{4\pi^2} K_{eff} \tag{18}$$

It should be noted that the mass is assigned as lumped to the corner nodes at the storey level. The average maximum lateral displacement $\Delta_{m,NTHA}$ of the selected frame is obtained from the results of the nonlinear time history analysis using the 10 ground motions. $\Delta_{m,NTHA}$ is compared with Δ_m. If the difference is within a 3% tolerance, the assigned mass is adopted for the given ductility. If the difference is above 3% tolerance, the effective mass is revised and the procedure is repeated. With the effective mass and the effective stiffness, the effective period T_{eff} is determined using equation 19. From the average elastic response spectra, the equivalent viscous damping value could be read in terms of T_{eff} and Δ_m. It should be noted that the modified hysteretic damping is determined using equation 20, where the elastic viscos damping (ζ_{el}) is taken as 5%.

$$T_{eff} = 2\pi \sqrt{\frac{m_{eff}}{K_{eff}}} \tag{19}$$

$$\zeta_{hys} = \zeta_{eq} - \zeta_{el} \tag{20}$$

Figure 9 shows the hysteretic damping values modified by nonlinear time history analysis with respect to the ductility for the frames.

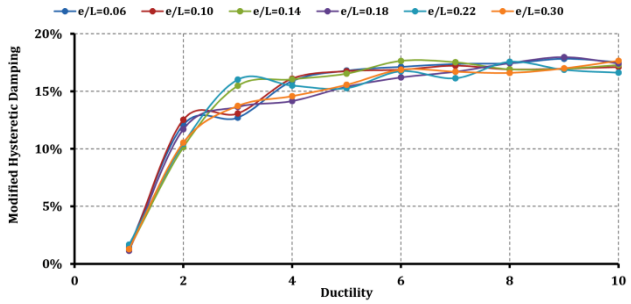

Fig. 10: Modified hysteretic damping against the ductility for EBF's

As shown in figure 10, the hysteretic damping obtained by the time history analysis is lower than the one calculated by Jacobsen method. In addition, it is shown that its value is mostly dependent on ductility and the effects of the link length to the span length ratio are negligible. To better illustrate the differences, the vertical axis of figure 11 indicates the ratio of the hysteretic damping obtained by the NTHA to hysteretic damping obtained by Jacobsen method. This figure illustrates that correction factors for all frames are decreased up to the ductility 2, and then approximately stay constant. For ductility levels greater than 2, the correction factor is close to 0.5.

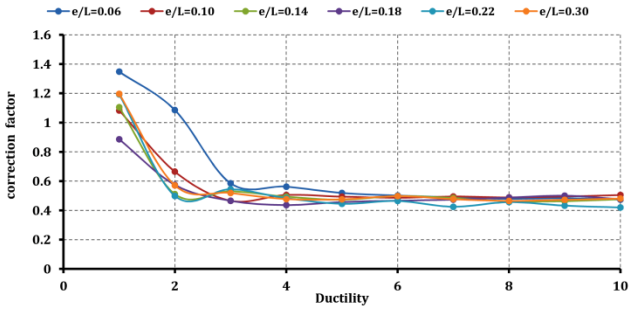

Fig. 11: Variation of Correction factor against ductility

Since the link length to the span length ratio has no significant effect on hysteretic damping, the mean value was used to find proper expression. Figure 12 illustrates the mean equivalent damping (ζ_{eq}) for six frames against the ductility and one calculated by standard expression (equation 3).

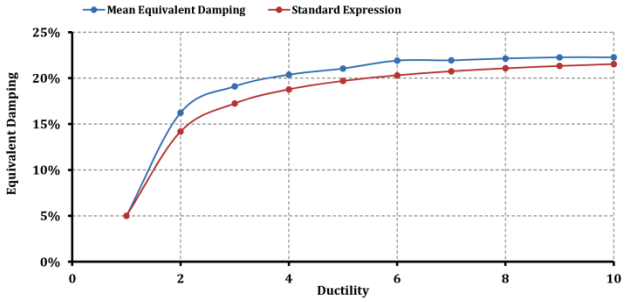

Fig. 12: Mean curve and damping obtained by standard expression

As shown in figure 12, the mean curve is almost close to standard expression. By modifying the coefficient C in equation 3, which is equal to 0.577 for all steel frames, to 0.635, it is still valid to use this equation for determining the equivalent damping. The fitted curve for EBF's is shown as a dashed line in figure 13, and obtained by the following expressions:

$$\zeta_{eq} = 0.05 + 0.635 \frac{\mu - 1}{\pi\mu} \tag{20}$$

As can be seen, the proposed equation based on modified standard expression is able to approximately estimate damping. Since this paper presents the criteria for designing EBF's according to the DDBD, the difference between the two estimates can be ignored and the proposed

expression can be used according to the design purpose. On the other hand, the multiple-degree-of-freedom structures are equalized as a single-degree-of-freedom system by the DDBD method. Therefore, the results of this study can be used to create a design based on the DDBD method.

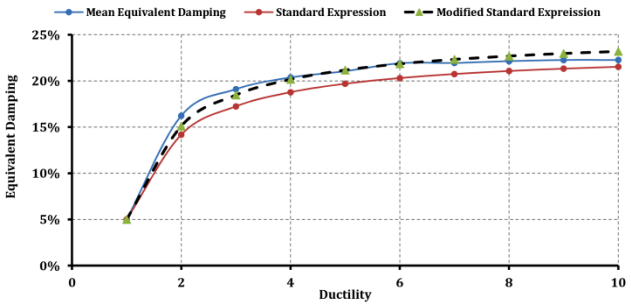

Fig. 13: Fitted curve for estimating equivalent damping of EBF's

8. Conclusions

In this study, the revised effective mass (REM) method was adopted in order to evaluate the Jacobsen method for calculating the damping in EBF systems. In this method, the yield displacement was determined using a proposed expression. Jacobsen damping was obtained from the displacement spectrum based on the target displacement and the effective period. Subsequently, the effective mass was estimated and nonlinear time history analyses were conducted until the convergence between the target displacement and the average displacement occurred. Eventually, by using the finalized effective mass, the effective period and the hysteretic damping were determined. Furthermore, the effects of link beam length, material, and system ductility on the hysteretic damping were investigated. Results showed that the effects of link length were negligible and ductility was the main factor. As ductility increased, the hysteretic damping increased; however, its rate decreased after a while. In addition, damping obtained by the Jacobsen method was larger than the damping determined by the nonlinear time history analysis. By means of nonlinear time history analysis, the modified standard expression was proposed to estimate equivalent damping of EBF's.

References

[1] Priestley, M. J. N (1993). "Myths and Fallacies in Earthquake Engineering Conflicts between design and Reality", *Bulletin of the New Zealand National Society for Earthquake Engineering*, Vol. 26, No. 3, PP. 329-341.

[2] Kowalsky, M.J., Priestley, M.J.N. and MacRae, G.A. (1994). "Displacement-based design: a methodology for seismic design applied to single degree of freedom reinforced concrete structures", *Structural Systems Research Report* 1994, University of California, San Diego.

[3] Calvi, G. M. and Kingsley, G. R. (1995). "Displacement-Based Seismic Design of Multi-Degree-of-Freedom Bridge Structures", *Earthquake Engineering and Structural Dynamics*, Vol. 24, PP. 1247-1266.

[4] Kowalsky, M. J. (2002). "A Displacement-Based Approach for the Seismic Design of Continuous Bridges", *Earthquake Engineering and Structural Dynamics*, Vol. 31 No. 3, PP. 719-747.

[5] Priestley, M. J. N. and Calvi, G. M. (2003). "Direct Displacement-Based Seismic Design of Concrete Bridges" *ACI 2003 International Conference: Seismic Bridge Design And Retrofit for Earthquake Resistance*, December 8-9, 2003, La Jolla, CA.

[6] Adhikari, G., Petrini, L. and Calvi, G. M. (2010). "Application of direct displacement based design to long span bridges", *Bulletin of Earthquake Engineering*, Vol. 8, No. 4, PP. 897-919.

[7] Calvi, G. M. and Pavese, A. (1995). "Displacement-Based Design of Building Structures" *European Seismic Design Practice: Research and Application, Proceedings of the Fifth SECED Conference*, Elnashai, A.S. (Ed.), Chester, United Kingdom, October 26-27 1995, A.A. Balkema, Rotterdam, PP. 127-132.

[8] Priestley, M. J. N. (1997). "Displacement-Based seismic assessment of reinforced concrete buildings", *Journal of Earthquake Engineering*, Vol. 1, No. 1, PP. 157-192.

[9] Harris, J L. (2004). "Comparison of steel moment frames designed in accordance with force-based and direct displacement-based design", *Proceedings SEAOC Convention*, August, Monterey, Canada.

[10] Yavas, A. (2006). "Displacement profile for displacement based design of dual frame systems", *4th International Conference on Earthquake Engineering*, Taipei, PP. 12-23, October 2006.

[11] Garcia, R., Sullivan, T. J. and Corte, G. D. (2010). "Development of a displacement-based design method for steel frame-Rc wall buildings", *Journal of Earthquake Engineering*, Vol. 14, No. 2, PP. 252-277.

[12] Wijesundara, K. K., Nascimbene, R. and Sullivan, T. J. (2011). "Equivalent viscous damping for steel concentrically braced frame structures", *Bulletin of earthquake engineering*, Vol. 9, No. 5, PP. 1535-1558.

[13] Yahyai, M. and Rezayibana, B. (2017). "New expressions to estimate damping in direct displacement based design for special concentrically-braced frames", *Numerical method in Civil Engineering*, Vol. 1, No. 3, PP. 34-45.

[14] Jacobsen, L. S. (1960). "Damping in composite structures.", In: Proceedings of 2nd world conference on

earthquake engineering, vol. 2, Tokyo and Kyoto, Japan, PP. 1029–1044.

[15] Dwairi, H. and Kowalsky, M. J. (2004). "Investigation of Jacobsen's equivalent viscous damping approach as applied to displacement-based seismic design", *Proceeding of 13th World Conference on Earthquake Engineering*, August 1-6 Vancouver, BC, Canada.

[16] Grant, D. N., Blandon, C. A. and Priestley, M. J. N. (2005). Modeling inelastic response in direct displacement-based design, Report 2005/03, IUSS Press, Pavia.

[17] Dwairi, H., Kowalsky, M. J. and Nau, J. M. (2007). "Equivalent damping in support of direct displacement-based design", *Journal of Earthquake Engineering*, Vol. 11, No. 4, PP. 512-530.

[18] Yahyai, M. and Rezayibana, B. (2015). "A Simplified Methodology to Determine Damping for Special Concentrically-Braced Frames", *International journal of steel structures*, Vol. 15, No. 3, PP. 541-555.

[19] AISC (2016). Seismic provisions for structural steel buildings, An American National Standard, ANSI/AISC 341-10, American Society of Civil Engineers, Chicago

[20] ABAQUS. 2012. ABAQUS Theory Manual and Users' Manual, Version 12.6. Hibbitt, Karlsson & Sorenson, Inc.

[21] Berman, J. W and Bruneau, M. (2007), "Experimental and analytical investigation of tubular links for eccentrically braced frames", *Engineering Structures* Vol. 29, No. 8, PP.1929-1938.

[22] ASCE (2010). Minimum design loads for buildings and other structures, An ASCE Standard, ASCE/SEI 7-10. American Society of Civil Engineers, Reston
Berkeley.

[23] Priestley, M. J. N., Calvi, G. M. and Kowalsky, M.J. Displacement-Based Design of Structures, 2007, IUSS